IEEE Photonics Journal
An IEEE Photonics Society Publication

Open Access

Experimental Demonstration of Amplified Feedback DFB Laser With Modulation Bandwidth Enhancement Based on the Reconstruction Equivalent Chirp Technique

Volume 9, Number 6, Deccember 2017

Jilin Zheng
Guowang Zhao
Yating Zhou
Zhike Zhang
Tao Pu
Yuechun Shi
Yunshan Zhang
Yu Liu
Lianyan Li
Jun Lu
Xing Zhang
Jin Li
Yuke Zhou
Xiangfei Chen, *Senior Member, IEEE*

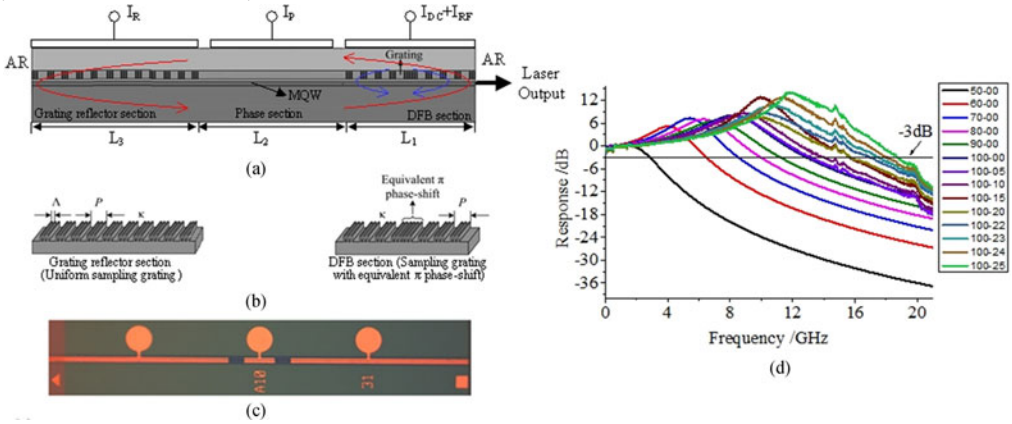

DOI: 10.1109/JPHOT.2017.2769963
1943-0655 © 2017 IEEE

Experimental Demonstration of Amplified Feedback DFB Laser With Modulation Bandwidth Enhancement Based on the Reconstruction Equivalent Chirp Technique

Jilin Zheng,[1] **Guowang Zhao**,[2] **Yating Zhou**,[3] **Zhike Zhang**,[4] **Tao Pu**,[1] **Yuechun Shi**,[2] **Yunshan Zhang**,[5,6] **Yu Liu**,[4] **Lianyan Li**,[5] **Jun Lu**,[2] **Xing Zhang**,[7] **Jin Li**,[1] **Yuke Zhou**,[2] **and Xiangfei Chen**,[2] ***Senior Member, IEEE***

[1]College of Communications Engineering, PLA Army Engineering University, Nanjing 210007, China
[2]College of Engineering and Applied Sciences, Nanjing University, Nanjing 210093, China
[3]School of Mathematics and Physics and Chemical Engineering, Changzhou Institute of Technology, Changzhou 213032, China
[4]Institute of Semiconductors, Chinese Academy of Sciences, Beijing 100083, China
[5]School of Optoelectronic Engineering, Nanjing University of Posts and Telecommunications, Nanjing 210023, China
[6]Nanjing University (Suzhou) High-Tech Institute, Suzhou 215123, China
[7]Changchun Institute of Optics and Fine Mechanics and Physics, Chinese Academy of Science, Changchun 130033, China

DOI:10.1109/JPHOT.2017.2769963

Manuscript received September 19, 2017; revised October 28, 2017; accepted November 1, 2017. Date of publication November 8, 2017; date of current version November 15, 2017. This work was supported in part by the National Natural Science Foundation of China for the Youth under Grants 61504170 and 61504058, in part by the Nature Science Foundation of Jiangsu Province for the Youth under Grants BK20140414, BK20160907, and BK20141168, in part by the National Natural Science Foundation of China under Grants 61435014, 11574141, 61575186, 61635001, and 61640419, in part by the Fundamental Research Funds for the Central Universities under Grant 021314380092, and in part by the National "863" Project of China under Grant 2015AA016902. Corresponding author: Yunshan Zhang (e-mail: zys5014@163.com).

Abstract: A novel amplified feedback DFB laser with extended modulation bandwidth is experimentally demonstrated in this paper. All the three sections of laser cavity, including DFB section, phase section, and amplified feedback section, have the same active layer, which can avoid the butt-joint regrowth process. The gratings in both DFB section and amplified feedback section are fabricated by the reconstruction equivalent chirp technique, which can significantly decrease the difficulties in realizing precise grating structure. An enhanced −3 dB bandwidth of 19 GHz is achieved by means of a normal low-frequency wafer. Modulation linearity and relative intensity noise characteristics are experimentally investigated. 20 MSymbol/s 32-QAM signal with 19 GHz carrier is transmitted via 25-km radio-over-fiber link using the as-fabricated directly modulated DFB laser, and the average error vector magnitude of the whole link is 3.91%.

Index Terms: DFB laser, amplified feedback, modulation bandwidth, reconstruction equivalent chirp, radio-over-fiber.

1. Introduction

High-bandwidth directly modulated semiconductor lasers (DML) are of great importance to many applications, such as optical communications, radio-over-fiber (ROF) links, modern radar systems, and so on [1]–[4]. Generally, the direct modulation bandwidth (MBW) of a DML is largely limited by the relaxation oscillation frequency. In order to extend the MBW, many efforts have been made including increasing the carrier-photon (CP) resonance frequency [1], [5] and taking advantage of the photon-photon resonance (PPR) effect [6]–[9]. Usually, the former approach is to optimize the differential gain of the multi-quantum well (MQW) active layer and shortening the laser length. While the latter option is achieved by optical-injection locking a directly modulated slave laser [7] or by optical feedback through an integrated optical waveguide [8]–[11]. As to the optical feedback mechanism, there exist two kinds: passive feedback [8], [9] and active/amplified feedback [10], [11]. Generally speaking, the former one needs butt-joint re-growth process to achieve active-passive integration, which may significantly increase the fabrication complexity. While for the latter one, some of the detailed realization solution also needs active-passive integration (phase section), some suffers from severe single-mode instability since the reflection is not wavelength-selective, and some need extremely sophisticated fabrication schemes (e.g., the E-beam lithography technique) to guarantee uniformity between the distributed feedback (DFB) section and the reflection grating section, which has not been experimentally confirmed yet [11]. Actually, to simplify the fabrication process of semiconductor lasers, many other previous work have been made including employing identical epitaxial layer (IEL) scheme [12], [13] to realize electroabsorption modulated lasers (EMLs), which can avoid butt-joint re-growth integration, and using surface gratings [14], [15] to realize DFB lasers that are regrowth free. Therefore, similar to these efforts, it is highly required to simplify the fabrication process of optical-feedback DFB laser with modulation bandwidth enhancement.

In this paper, a novel amplified feedback DFB (AF-DFB) laser with enhanced MBW is experimentally demonstrated. In this structure, all the three sections of laser cavity, including DFB section, phase section and amplified feedback section, have the same active layer, which can avoid the butt-joint re-growth process. Meanwhile, the gratings in both DFB section and amplified feedback section are fabricated by the Reconstruction Equivalent Chirp (REC) technique [16], which can significantly decrease the difficulties in realizing precise grating structure. An enhanced -3 dB bandwidth of 19 GHz is achieved by means of a normal low-frequency wafer. Modulation linearity and relative intensity noise (RIN) characteristics are experimentally investigated. 20 MSymbol/s 32-QAM signal with 19 GHz carrier are transmitted via 25 km radio-over-fiber link using the as-fabricated directly modulated DFB laser, and the average error vector magnitude (EVM) of the whole link is 3.91%.

2. Laser Device Design

The structure of the AF-DFB laser is schematically shown in Fig. 1. It consists of three sections, including the DFB section, the phase section and the grating reflector section, which are electrically isolated each other. All these three sections have the same active layer and have different separated injection current. The radio frequency (RF) to be modulated is loaded at the DFB section. The lengths of these three sections are (from right to left) 500 μm, 100 μm and 500 μm, respectively. The epitaxy is grown by conventional two-stage metal organic chemical vapor deposition (MOCVD). An n-InP buffer layer, an n-InAlGaAs lower optical confinement layer, an InAlGaAs multiple-quantum-well (MQW) structure, a p-InAlGaAs upper optical confinement layer and a p-InAlGaAs grating layer are successively grown on an n-InP substrate in the first epitaxial growth. The MQW structure contains five 6 nm-thick 1.2% compressive-strain AlGaInAs wells separated by six 9 nm-thick -0.45% tensile-strain InGaAsP barriers. The photoluminescence (PL) peak of the MQW is around 1535 nm at room temperature, which is shown in Fig. 1(d). The gratings in both DFB section and amplified feedback section are fabricated by the REC Technique by means of sampled grating pattern that is formed by a conventional holographic exposure combining with a conventional photolithography [16]. Both gratings in the two sections have identical seed grating period Λ that is determined by holographic exposure, while the sampling period function P determines the required

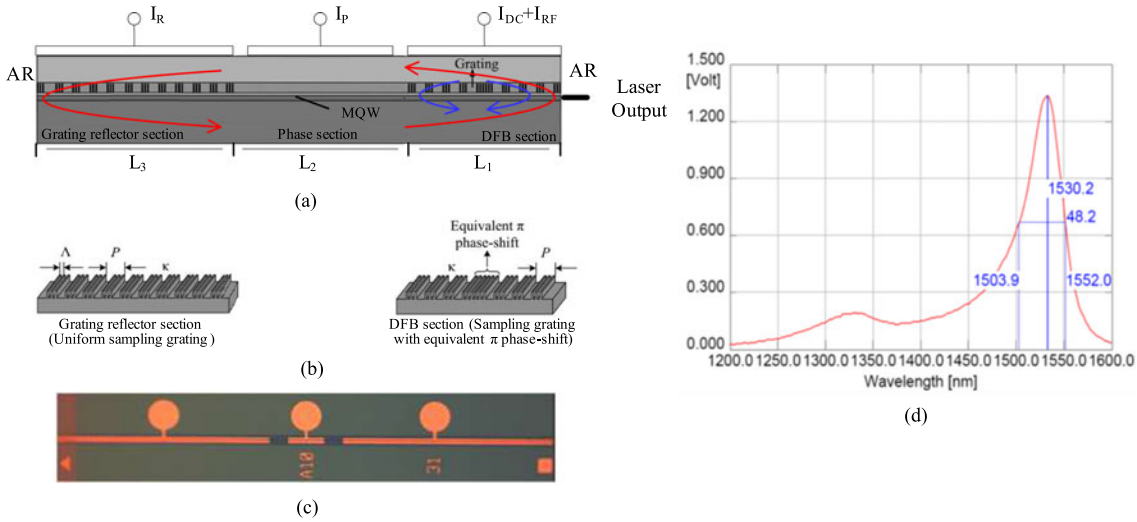

Fig. 1. Laser device: (a) schematic of laser structure, (b) REC grating structure, (c) photograph of laser chip, and (d) PL spectrum of the MQW.

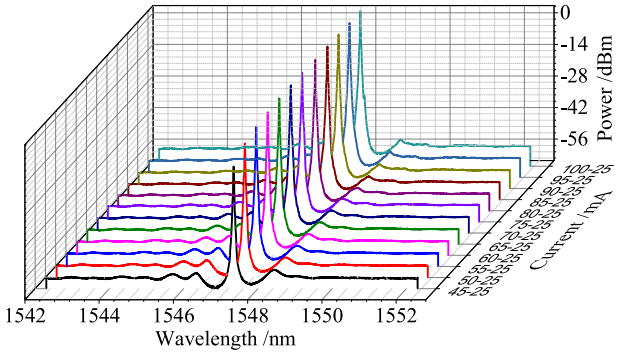

Fig. 2. Measured spectrum with I_{DC} being varied from 45 to 100 mA while I_R being fixed at 25 mA. The title of *Z*-axis is according to the format of "$I_{DC}-I_R$".

sophisticate grating structure, such as the detailed operation wavelength and equivalent π phase-shift, the principle of which can be found in Ref. [17]. In this work, the Λ and P are designed to be 256.644 nm and 4.155 μm, respectively. Both facets of the devices are anti-reflection (AR) coated with reflectivity less than 1%. The photograph of fabricated laser chip is shown in Fig. 1(c).

3. Experimental Results

The AF-DFB laser chip is packaged in butterfly housing as a module for measurement. Both the optical spectrum and small-signal modulation response are tested under different injection current. In this work, the current of phase section I_P is fixed at 0 mA, while I_{DC} and I_R are varied to testify the mode stability and PPR effect.

3.1 Optical Spectrum Under Different Cunrrent

First, I_{DC} is varied from 45 to 100 mA while I_R is fixed at 25 mA, the measured spectrum are shown in Fig. 2. The results show good single-mode stability with side mode suppression ratio (SMSR) larger than 35 dB. Second, I_R is varied from 0 to 30 mA while I_{DC} is fixed at 100 mA, the measured

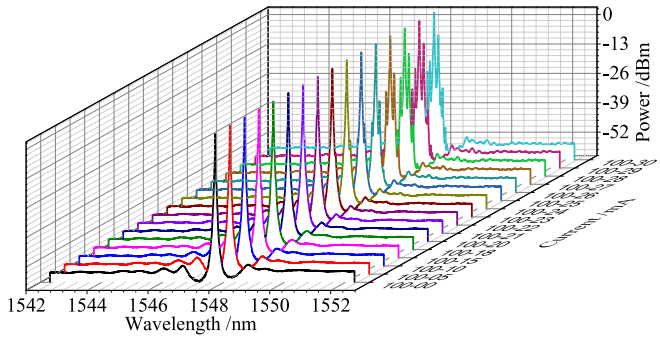

Fig. 3. Measured spectrum with I_R being varied from 0 to 30 mA while I_{DC} being fixed at 100 mA.

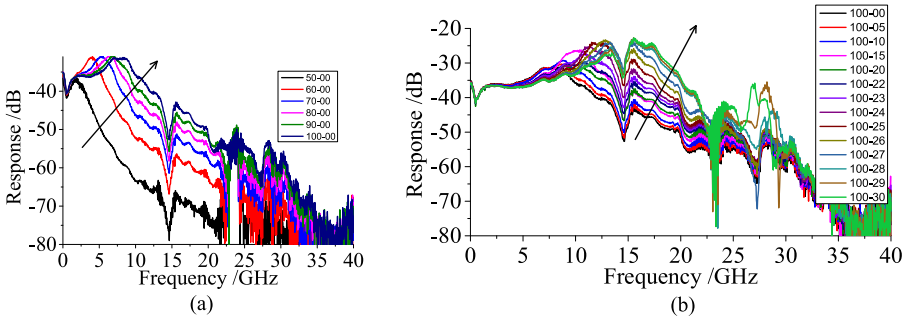

Fig. 4. Measured frequency responses under different currents: (a) with I_{DC} being varied only and (b) with I_R being varied only.

spectrum are shown in Fig. 3. The results show that when I_R is larger than 26 mA, this laser works at a multi-mode emission with SMSR decreasing rapidly. This result provides a good suggestion for choosing proper working currents to take advantage of PPR effect.

3.2 Small-Signal Modulation Response Under Different Current

We employ a vector network analyzer (VNA: R&SZVA67) and a high-speed photodetector (PD: U2T XPDV 2120 R) to test the small-signal modulation frequency responses of the AF-DFB laser module at different currents, which are shown in Fig. 4. Fig. 4(a) shows that MBW of such a DML increases with the increase of I_{DC}, which is attributed to the improved CP resonance frequency. While Fig. 4(b) shows that MBW gets enhanced further with the increase of I_R, which benefits from the PPR effect. Taking into account of the single-mode stability, the −3 dB MBW of such a single-mode laser reaches up to 19 GHz under the current of "100-25", while the −3 dB MBW of the free-running laser without amplified feedback current I_R is about 11.4 GHz (i. e., the current state of "100-00"). It should be noted that the final S21 curves of such a laser module has get deteriorated by the extrinsic parasitic network including package response. However, the extrinsic effects of the parasitic network are independent from the current imposed on laser chip. So, we can remove the extrinsic effects of the parasitic network by subtracting the measured frequency response from two different bias levels. Actually, the intrinsic response of laser chip can be extracted from the measured frequency response curves using the reported methods [18], [19]. After obtaining the intrinsic response of laser chip, extrinsic response curve can be derived by subtracting the intrinsic response from measured frequency response. The extrinsic response of the parasitic network and the intrinsic response of laser chip under different current are shown in Fig. 5. Fig. 5(a) shows clearly that the strong notches near 15 GHz in the frequency response curves of Fig. 4(b) stem from the extrinsic effects of the parasitic network mainly caused by the package. Fig. 5(b) shows

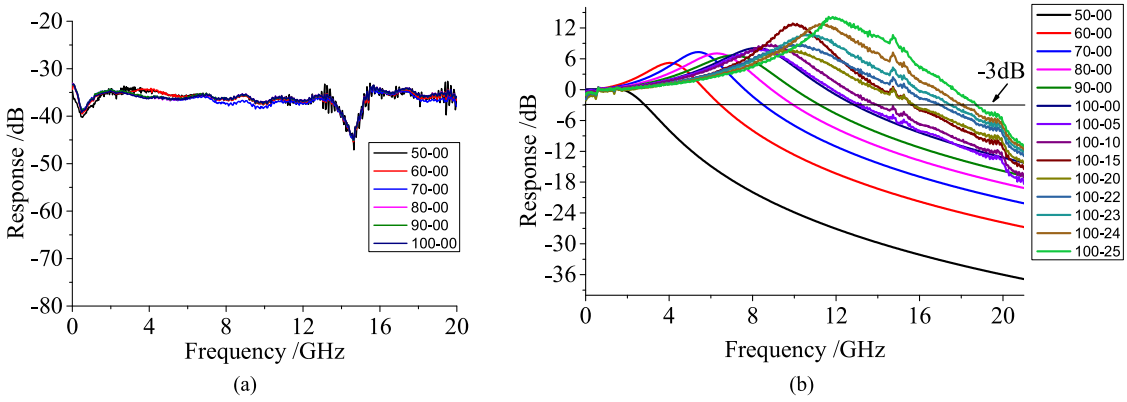

Fig. 5. (a) Extrinsic response of the parasitic network under different currents. (b) Intrinsic response of laser chip under different currents.

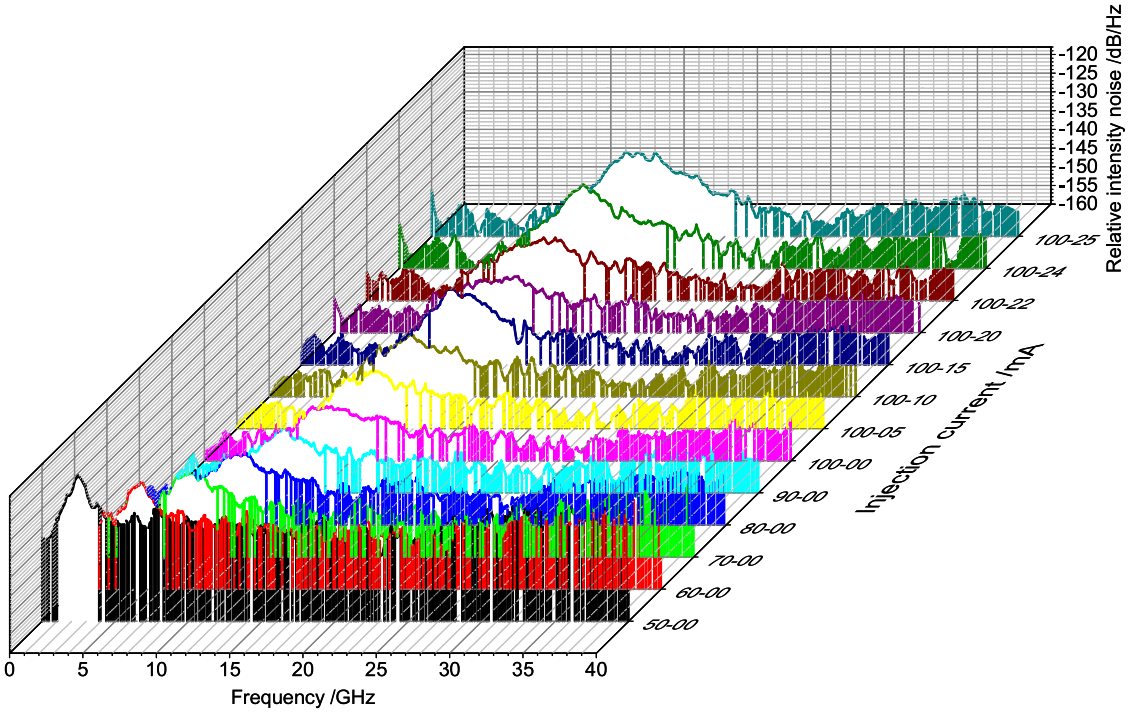

Fig. 6. The evolution process of RIN under different currents.

that the intrinsic −3 dB MBW of laser chip without amplified feedback current I_R (i. e., the current state of "100-00") is about 12.8 GHz, while the intrinsic −3 dB MBW of AF-DFB laser chip under the current of "100-25" gets enhanced to 19.1 GHz, which indicates that PPR effect has successfully enhanced the MBW of a laser chip.

3.3 RIN Characteristics and Modulation Linearity

RIN describes fluctuations in the optical power of a laser, which mainly determines the noise level for a DML. In this work, the RIN of the proposed AF-DFB laser was measured under different bias currents utilizing the method demonstrated in Ref. [20]. Fig. 6 shows the experimental results.

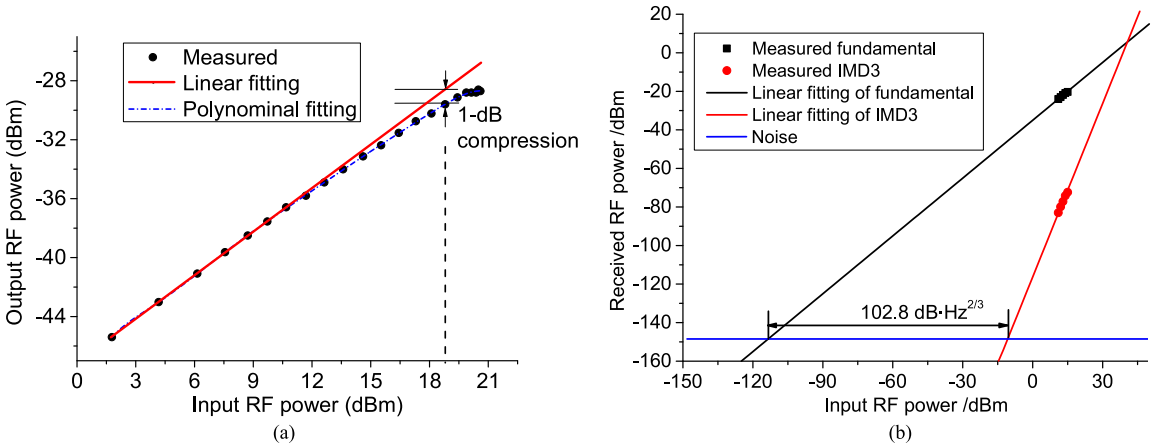

Fig. 7. (a) The measured 1-dB compression point of the AF-DFB laser. (b) The measured SFDR of the AF-DFB laser.

The entire evolution process of RIN under different currents reflects two important characteristics. The first one is that when the grating reflector section has no current injected, the value of RIN decreases with the increase of current imposed on DFB section while the RIN peak position moves to high frequency; the second one is that when the current imposed on DFB section keeps fixed, as the reflector's current is increased, the RIN peak position moves to high frequency further and its width gets wider. This phenomenon is attributed to the PPR effect, which also agrees well with the intrinsic response of laser chip as shown in Fig. 5(b). Note that under the current of "100-25", the RIN in the relaxation oscillation frequency (~14 GHz) and in 19 GHz is about −137.8 dB/Hz and −148.5 dB/Hz, respectively.

Modulation linearity is one of the most important performances for an analog DML. In this work, the 1-dB compression point and spurious free dynamic range (SFDR) of such an AF-DFB laser were measured, respectively. The AF-DFB laser worked under the current of "100-25", and the DFB section was directly modulated by a single tone 19-GHz RF signal and a two-tone RF signal with frequencies of 19 GHz and 19.02 GHz for 1-dB compression point and SFDR tests, respectively. An electrical spectrum analyzer (ESA) was used to measure the output RF power from a photo-detector (PD) that detects the modulated optical signal. Fig. 7(a) plots the output RF power against input RF power modulating AF-DFB laser. The results show that the output RF power deviates from the linear fitting curve when the input RF power gets increased large enough, which finally results in 1-dB dropping at the very input RF power named 1-dB compression point. As to such an AF-DFB laser, the 1-dB compression point occurs at 18.8 dBm. The SFDR of AF-DFB laser around 19 GHz is also measured taking the RIN in 19 GHz as the noise floor, which is shown in Fig. 7(b). After fitting and extrapolating, the SFDR is calculated to be 102.8 $dB \cdot Hz^{2/3}$.

3.4 Application in ROF Link

Finally, to test the transmission performance of the as-fabricated directly modulated DFB laser, 20 MSymbol/s 32-QAM signal with 19 GHz carrier are transmitted via 25 km radio-over-fiber link using this laser module, and the setup is shown in Fig. 8. The laser worked under the current of "100-25". The 0.5 GHz 20 MSymbol/s 32-QAM signal was generated by an Agilent E4438C ESG Vector Signal Generator. Then the 32-QAM signal was up-converted to 19 GHz by a wideband mixer with a 19.5 GHz RF generated by Anritsu MG3694B Signal Generator. At last, the electrical signal from the PIN detector was transmitted to the Signal Analyzer (Rohde&Schwarz FPS 30) for demodulation and analysis. Fig. 9 shows the analysis results. The results clearly indicate that the received constellation diagram is good and the average EVM of the whole link is 3.91%.

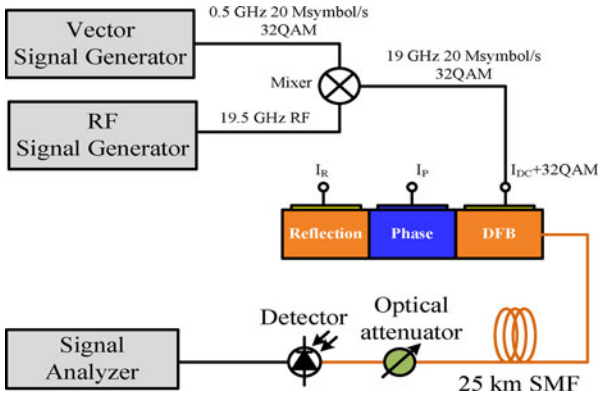

Fig. 8. Schematic of ROF link using the laser module.

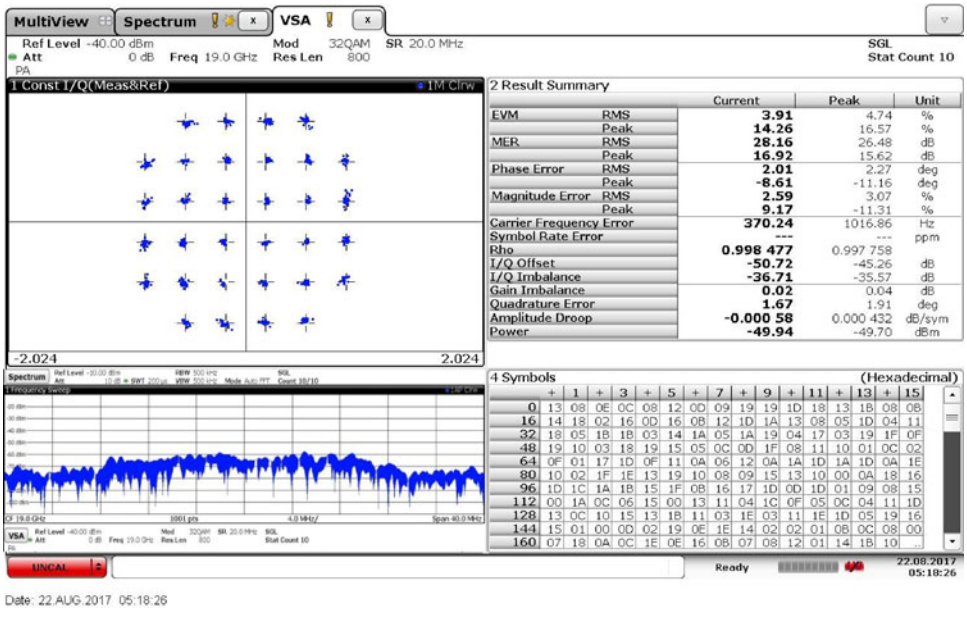

Fig. 9. Analysis of the received signal.

4. Conclusion

We experimentally demonstrate a novel AF-DFB laser with extended modulation bandwidth up to 19 GHz using a normal low-frequency wafer. The amplified feedback structure of this laser, which can avoid the butt-joint re-growth process, can enhance the performance of modulation response by taking advantage of PPR effects. Furthermore, the sophisticated gratings in laser cavity can be formed by conventional holographic exposure combining with a conventional photolithography benefitting from the REC technique. The measured results of RIN characteristics, modulation linearity and ROF link test confirm the performance of the as-fabricated directly modulated DFB laser. It should be noted that the enhancement reported in this paper (i. e., the -3 dB MBW gets enhanced from 12.8 GHz to 19.1 GHz) doesn't bring along giant achievement compared with others' research works, however, in the future work we can further improve the performance of such a novel AF-DFB laser by optimizing the laser structure, e. g., shortening the length of DFB section instead of current 500 μm long. Hence, this work provides a novel low-cost solution to realizing high-performance DMLs.

References

[1] K. Nakahara *et al.*, "40-Gb/s direct modulation with high extinction ratio operation of 1.3-μm InGaAlAs multiquantum well ridge waveguide distributed feedback lasers," *IEEE Photon. Technol. Lett.*, vol. 19, no. 19, pp. 1436–1438, Oct. 2007.

[2] A. Kaszubowska, P. Anandarajah, and L. P. Barry, "Improved performance of a hybrid radio/fiber system using a directly modulated laser transmitter with external injection," *IEEE Photon. Technol. Lett.*, vol. 14, no. 2, pp. 233–235, Feb. 2002.

[3] H.-H. Lu, H.-H. Huang, H.-S. Su, and M.-C. Wang, "Fiber optical CATV system-performance improvement by using external light-injection technique," *IEEE Photon. Technol. Lett.*, vol. 15, no. 7, pp. 1017–1019, Jul. 2003.

[4] R. A. York and T. Itoh, "Injection- and phase-locking techniques for beam control antenna arrays," *IEEE Trans. Microw. Theory Techn.*, vol. 46, no. 11, pp. 1920–1929, Nov. 1998.

[5] L. Xie *et al.*, "24-GHz directly modulated DFB laser modules for analog applications," *IEEE Photon. Technol. Lett.*, vol. 24, no. 5, pp. 407–409, Mar. 2012.

[6] J. P. Reithmaier *et al.*, "Modulation speed enhancement by coupling to higher order resonances: A road towards 40 GHz bandwidth lasers on InP," in *Proc. Indium Phosphide Relat. Mater.*, 2005, pp. 118–123.

[7] E. K. Lau, X. Zhao, C. Chang-Hasnain, and M. C. Wu, "80-GHz intrinsic 3-dB bandwidth of directly modulated semiconductor lasers under optical injection locking," in *Proc. Int. Semicond. Laser Conf.*, 2008, pp. 171–172.

[8] M. Radziunas *et al.*, "Improving the modulation bandwidth in semiconductor lasers by passive feedback," *IEEE J. Sel. Topics Quantum Electron.*, vol. 13, no. 1, pp. 136–142, Jan./Feb. 2007.

[9] J. Kreissl, V. Vercesi, U. Troppenz, T. Gaertner, W. Wenisch, and M. Schell, "Up to 40 Gb/s directly modulated laser operating at low driving current: Buried-heterostructure passive feedback laser (BH-PFL)," *IEEE Photon. Technol. Lett.*, vol. 24, no. 5, pp. 362–364, Mar. 2012.

[10] L. Yu, L. Guo, D. Lu, C. Ji, H. Wang, and L. Zhao, "Modulated bandwidth enhancement in an amplified feedback laser," *Chin. Opt. Lett.*, vol. 13, 2015, Art. no. 051401.

[11] G. Zhao, J. Sun, Y. Xi, D. Gao, Q. Lu, and W. Guo, "Design and simulation of two-section DFB lasers with short active-section lengths," *Opt. Express*, vol. 24, pp. 10590–10598, 2016.

[12] L. Hou, M. Tan, M. Haji, I. Eddie, and J. H. Marsh, "EML based on side-wall grating and identical epitaxial layer scheme," *IEEE Photon. Technol. Lett.*, vol. 25, no. 12, pp. 1169–1172, Jun. 2013.

[13] C. Sun *et al.*, "Fabrication and packaging of 40-Gb/s AlGaInAs multiple-quantum-well electroabsorption modulated lasers based on identical epitaxial layer scheme," *J. Lightw. Technol.*, vol. 26, no. 11, pp. 1464–1471, Jun. 2008.

[14] H. S. Djie, H. S. Djie, C. Sookdhis, and P. Dowd, "Analysis and modeling of distributed feedback and distributed Bragg reflector lasers using regrowth-free index-coupled surface grating technology," *Opt. Eng.*, vol. 41, pp. 2345–2352, 2002.

[15] J. Fricke *et al.*, "High-power distributed feedback lasers with surface gratings," *IEEE Photon. Technol. Lett.*, vol. 24, no. 16, pp. 1443–1445, Aug. 2012.

[16] Y. Shi *et al.*, "High channel count and high precision channel spacing multi-wavelength laser array for future PICs," *Sci. Rep.*, vol. 4, 2014, Art. no. 7377.

[17] Y. Dai and X. Chen, "DFB semiconductor lasers based on reconstruction-equivalent-chirp technology," *Opt. Express*, vol. 15, pp. 2348–2353, 2007.

[18] J. H. Han and S. W. Park, "Experimental study of a hybrid small-signal parameter modeling and extraction method for a microoptoelectronic device," *IEEE/ASME Trans. Mechatronics*, vol. 20, no. 6, pp. 3285–3290, Dec. 2015.

[19] J. C. Cartledge and R. C. Srinivasan, "Extraction of DFB laser rate equation parameters for system simulation purposes," *J. Lightw. Technol.*, vol. 15, no. 5, pp. 852–860, May 1997.

[20] P. Anandarajah, S. Latkowski, C. Browning, R. Zhou, J. O'Carroll, and R. Phelan, "Integrated two-section discrete mode laser," *IEEE Photon. J.*, vol. 4, no. 6, pp. 2085–2094, Dec. 2012.